

# Absolute pulse energy measurements of soft x-rays at the Linac Coherent Light Source

K. Tiedtke,<sup>1</sup> A. A. Sorokin,<sup>1,2</sup> U. Jastrow,<sup>1</sup> P. Juranić,<sup>1</sup> S. Kreis,<sup>1</sup> N. Gerken,<sup>3</sup>  
M. Richter,<sup>4</sup> U. Arp,<sup>5</sup> Y. Feng,<sup>6</sup> D. Nordlund,<sup>7</sup> R. Soufli,<sup>8</sup> M. Fernández-Perea,<sup>8,9</sup>  
L. Juha,<sup>10</sup> P. Heimann,<sup>6</sup> B. Nagler,<sup>6</sup> H. J. Lee,<sup>6</sup> S. Mack,<sup>11</sup> M. Cammarata,<sup>6</sup> O. Krupin,<sup>6</sup>  
M. Messerschmidt,<sup>6,12</sup> M. Holmes,<sup>6</sup> M. Rowen,<sup>6</sup> W. Schlotter,<sup>6</sup> S. Moeller,<sup>6</sup>  
and J. J. Turner<sup>6,\*</sup>

<sup>1</sup>Deutsches Elektronen-Synchrotron, DESY, Notkestrasse 85, D-22603 Hamburg, Germany

<sup>2</sup>Ioffe Physico-Technical Institute, Polytekhnicheskaya 26, 194021 St Petersburg, Russia

<sup>3</sup>Universität Hamburg, Institut für Experimentalphysik, Luruper Chaussee 149, 22761 Hamburg, Germany

<sup>4</sup>Physikalisch-Technische Bundesanstalt, PTB, Abbestr. 2-12, D-10587 Berlin, Germany

<sup>5</sup>National Institute of Standards and Technology, 100 Bureau Drive, Stop 1070, Gaithersburg, MD 20899-1070, USA

<sup>6</sup>Linac Coherent Light Source, SLAC National Accelerator Laboratory, 2575 Sandhill Rd, Menlo Park, CA 94025 USA

<sup>7</sup>Stanford Synchrotron Radiation Lightsource, SLAC National Accelerator Laboratory, 2575 Sand Hill Rd, Menlo Park, CA 94025 USA

<sup>8</sup>Lawrence Livermore National Laboratory, 7000 East Avenue, Livermore, CA 94550 USA

<sup>9</sup>Consejo Superior de Investigaciones Científicas, C/ Serrano 144, 28006 Madrid, Spain

<sup>10</sup>Institute of Physics, Academy of Sciences of the Czech Republic, Na Slovance 2, 182 21 Prague 8, Czech Republic

<sup>11</sup>Physics Department, University of California at Berkeley, Berkeley, CA 94720 USA

<sup>12</sup>National Science Foundation BioXFEL Science and Technology Center, 700 Ellicott Street, Buffalo, New York 14203 USA

\*[joshuat@slac.stanford.edu](mailto:joshuat@slac.stanford.edu)

**Abstract:** This paper reports novel measurements of x-ray optical radiation on an absolute scale from the intense and ultra-short radiation generated in the soft x-ray regime of a free electron laser. We give a brief description of the detection principle for radiation measurements which was specifically adapted for this photon energy range. We present data characterizing the soft x-ray instrument at the Linac Coherent Light Source (LCLS) with respect to the radiant power output and transmission by using an absolute detector temporarily placed at the downstream end of the instrument. This provides an estimation of the reflectivity of all x-ray optical elements in the beamline and provides the absolute photon number per bandwidth per pulse. This parameter is important for many experiments that need to understand the trade-offs between high energy resolution and high flux, such as experiments focused on studying materials via resonant processes. Furthermore, the results are compared with the LCLS diagnostic gas detectors to test the limits of linearity, and observations are reported on radiation contamination from spontaneous undulator radiation and higher harmonic content.

©2014 Optical Society of America

**OCIS codes:** (120.0120) Instrumentation, measurement, and metrology; (320.0320) Ultrafast optics.

---

## References and links

1. J. Feldhaus, J. Arthur, and J. B. Hastings, "X-ray free-electron lasers," *J. Phys. At. Mol. Opt. Phys.* **38**(9), S799–S819 (2005).
2. W. Ackermann, G. Asova, V. Ayvazyan, A. Azima, N. Baboi, J. Bähr, V. Balandin, B. Beutner, A. Brandt, A. Bolzmann, R. Brinkmann, O. I. Brovko, M. Castellano, P. Castro, L. Catani, E. Chiadroni, S. Choroba, A. Cianchi, J. T. Costello, D. Cubaynes, J. Dardis, W. Decking, H. Delsim-Hashemi, A. Delsérieys, G. Di Pirro, M. Dohlus, S. Düsterer, A. Eckhardt, H. T. Edwards, B. Faatz, J. Feldhaus, K. Flöttmann, J. Frisch, L. Fröhlich, T. Garvey, U. Gensch, Ch. Gerth, M. Görler, N. Golubeva, H.-J. Grabosch, M. Grecki, O. Grimm, K. Hacker, U.

- Hahn, J. H. Han, K. Honkavaara, T. Hott, M. Hüning, Y. Ivanisenko, E. Jaeschke, W. Jalmuzna, T. Jezynski, R. Kammering, V. Katalev, K. Kavanagh, E. T. Kennedy, S. Khodyachykh, K. Klose, V. Kocharyan, M. Körfer, M. Kollwe, W. Koprek, S. Korepanov, D. Kostin, M. Krassilnikov, G. Kube, M. Kuhlmann, C. L. S. Lewis, L. Lilje, T. Limberg, D. Lipka, F. Löhler, H. Luna, M. Luong, M. Martins, M. Meyer, P. Michelato, V. Miltchev, W. D. Möller, L. Monaco, W. F. O. Müller, O. Napieralski, O. Napoly, P. Nicolosi, D. Nölle, T. Nunez, A. Oppelt, C. Pagani, R. Paparella, N. Pchalek, J. Pedregosa-Gutierrez, B. Petersen, B. Petrosyan, G. Petrosyan, L. Petrosyan, J. Pflüger, E. Plönjes, L. Poletto, K. Pozniak, E. Prat, D. Proch, P. Pucyk, P. Radcliffe, H. Redlin, K. Rehlich, M. Richter, M. Roehrs, J. Roensch, R. Romaniuk, M. Ross, J. Rossbach, V. Rybnikov, M. Sachwitz, E. L. Saldin, W. Sandner, H. Schlarb, B. Schmidt, M. Schmitz, P. Schmüser, J. R. Schneider, E. A. Schneidmiller, S. Schnepf, S. Schreiber, M. Seidel, D. Sertore, A. V. Shabunov, C. Simon, S. Simrock, E. Sombrowski, A. A. Sorokin, P. Spanknebel, R. Spesyvtsev, L. Staykov, B. Steffen, F. Stephan, F. Stulle, H. Thom, K. Tiedtke, M. Tischer, S. Toleikis, R. Treusch, D. Trines, I. Tsakov, E. Vogel, T. Weiland, H. Weise, M. Wellhöfer, M. Wendt, I. Will, A. Winter, K. Wittenburg, W. Wurth, P. Yeates, M. V. Yurkov, I. Zagorodnov, and K. Zapfe, "Operation of a free electron laser from the extreme ultraviolet to the water window," *Nat. Photonics* **1**(6), 336–342 (2007).
3. T. Shintake, H. Tanaka, T. Hara, T. Tanaka, K. Togawa, M. Yabashi, Y. Otake, Y. Asano, T. Bizen, T. Fukui, S. Goto, A. Higashiyama, T. Hirono, N. Hosoda, T. Inagaki, S. Inoue, M. Ishii, Y. Kim, H. Kimura, M. Kitamura, T. Kobayashi, H. Maesaka, T. Masuda, S. Matsui, T. Matsushita, X. Marchal, M. Nagasono, H. Ohashi, T. Ohata, T. Ohshima, K. Onoe, K. Shirasawa, T. Takagi, S. Takahashi, M. Takeuchi, K. Tamasaku, R. Tanaka, Y. Tanaka, T. Tanikawa, T. Togashi, S. Wu, A. Yamashita, K. Yanagida, C. Zhang, H. Kitamura, and T. Ishikawa, "A compact free-electron laser for generating coherent radiation in the extreme ultraviolet region," *Nat. Photonics* **2**(9), 555–559 (2008).
  4. P. Emma, R. Akre, J. Arthur, R. Bionta, C. Bostedt, J. Bozek, A. Brachmann, P. Bucksbaum, R. Coffee, F.-J. Decker, Y. Ding, D. Dowell, S. Edstrom, A. Fisher, J. Frisch, S. Gilevich, J. Hastings, G. Hays, P. Hering, Z. Huang, R. Iverson, H. Loos, M. Messerschmidt, A. Miahnahri, S. Moeller, H.-D. Nuhn, G. Pile, D. Ratner, J. Rzepiela, D. Schultz, T. Smith, P. Stefan, H. Tompkins, J. Turner, J. Welch, W. White, J. Wu, G. Yocky, and J. Galayda, "First lasing and operation of an ångström-wavelength free-electron laser," *Nat. Photonics* **4**(9), 589–591 (2010).
  5. E. Allaria, D. Castronovo, P. Cinquegrana, P. Craievich, M. Dal Forno, M. B. Danailov, G. D'Auria, A. Demidovich, G. De Nino, S. Di Mitri, B. Diviacco, W. M. Fawley, M. Ferianis, E. Ferrari, L. Froehlich, G. Gaio, D. Gauthier, L. Giannessi, R. Ivanov, B. Mahieu, N. Mahne, I. Nikolov, F. Parmigiani, G. Penco, L. Raimondi, C. Scafuri, C. Serpico, P. Sigalotti, S. Spampinati, C. Spezzani, M. Svandrlik, C. Svetina, M. Trovo, M. Veronese, D. Zangrando, and M. Zangrando, "Two-stage seeded soft-X-ray free-electron laser," *Nat. Photonics* **7**(11), 913–918 (2013).
  6. T. Ishikawa, H. Aoyagi, T. Asaka, Y. Asano, N. Azumi, T. Bizen, H. Ego, K. Fukami, T. Fukui, Y. Furukawa, S. Goto, H. Hanaki, T. Hara, T. Hasegawa, T. Hatsui, A. Higashiyama, T. Hirono, N. Hosoda, M. Ishii, T. Inagaki, Y. Inubushi, T. Itoga, Y. Joti, M. Kago, T. Kameshima, H. Kimura, Y. Kirihara, A. Kiyomichi, T. Kobayashi, C. Kondo, T. Kudo, H. Maesaka, X. M. Maréchal, T. Masuda, S. Matsubara, T. Matsumoto, T. Matsushita, S. Matsui, M. Nagasono, N. Nariyama, H. Ohashi, T. Ohata, T. Ohshima, S. Ono, Y. Otake, C. Saji, T. Sakurai, T. Sato, K. Sawada, T. Seike, K. Shirasawa, T. Sugimoto, S. Suzuki, S. Takahashi, H. Takebe, K. Takeshita, K. Tamasaku, H. Tanaka, R. Tanaka, T. Tanaka, T. Togashi, K. Togawa, A. Tokuhisa, H. Tomizawa, K. Tono, S. Wu, M. Yabashi, M. Yamaga, A. Yamashita, K. Yanagida, C. Zhang, T. Shintake, H. Kitamura, and N. Kumagai, "A compact X-ray free-electron laser emitting in the sub-ångström region," *Nat. Photonics* **6**(8), 540–544 (2012).
  7. M. Kato, N. Saito, T. Tanaka, Y. Morishita, H. Kimura, H. Ohashi, M. Nagasono, M. Yabashi, K. Tono, T. Togashi, A. Higashiyama, and T. Ishikawa, "Pulse energy of the extreme-ultraviolet free-electron laser at SPring-8 determined using a cryogenic radiometer," *Nucl. Instrum. Methods. A* **612**(1), 209–211 (2009).
  8. J. Bozek, "AMO instrumentation for the LCLS X-ray FEL," *Eur. Phys. J. Spec. Top.* **169**(1), 129–132 (2009).
  9. W. F. Schlotter, J. J. Turner, M. Rowen, P. Heimann, M. Holmes, O. Krupin, M. Messerschmidt, S. Moeller, J. Krzywinski, R. Soufli, M. Fernández-Perea, N. Kelez, S. Lee, R. Coffee, G. Hays, M. Beye, N. Gerken, F. Sorgenfrei, S. Hau-Riege, L. Juha, J. Chalupsky, V. Hajkova, A. P. Mancuso, A. Singer, O. Yefanov, I. A. Vartanyants, G. Cadenazzi, B. Abbey, K. A. Nugent, H. Sinn, J. Lüning, S. Schaffert, S. Eisebitt, W.-S. Lee, A. Scherz, A. R. Nilsson, and W. Wurth, "The soft x-ray instrument for materials studies at the linac coherent light source x-ray free-electron laser," *Rev. Sci. Instrum.* **83**(4), 043107 (2012).
  10. M. Richter, A. Gottwald, U. Kroth, A. Sorokin, S. Bobashev, L. Shmaenok, J. Feldhaus, C. Gerth, B. Steeg, K. Tiedtke, and R. Treusch, "Measurement of gigawatt radiation pulses from a vacuum and extreme ultraviolet free-electron laser," *Appl. Phys. Lett.* **83**(14), 2970–2972 (2003).
  11. M. Kato, T. Tanaka, T. Kurosawa, N. Saito, M. Richter, A. Sorokin, K. Tiedtke, T. Kudo, K. Tono, M. Yabashi, and T. Ishikawa, "Pulse energy measurement at the hard x-ray laser in Japan," *Appl. Phys. Lett.* **101**(2), 023503 (2012).
  12. S. Hau-Riege, R. Bionta, D. Ryutov, and J. Krzywinski, "Measurement of x-ray free-electron-laser pulse energies by photoluminescence in nitrogen gas," *J. Appl. Phys.* **103**(5), 053306 (2008).
  13. N. Saito, P. Juranic, M. Kato, M. Richter, A. Sorokin, K. Tiedtke, U. Jastrow, U. Kroth, H. Schöppe, M. Nagasono, M. Yabashi, K. Tono, T. Togashi, H. Kimura, H. Ohashi, and T. Ishikawa, "Radiometric comparison for measuring the absolute radiant power of a free-electron laser in the extreme ultraviolet," *Metrologia* **47**(1), 21–23 (2010).

14. S. Moeller, J. Arthur, A. Brachmann, R. Coffee, F.-J. Decker, Y. Ding, D. Dowell, S. Edstrom, P. Emma, Y. Feng, A. Fisher, J. Frisch, J. Galayda, S. Gilevich, J. Hastings, G. Hays, P. Hering, Z. Huang, R. Iverson, J. Krzywinski, S. Lewis, H. Loos, M. Messerschmidt, A. Miahnahri, H.-D. Nuhn, D. Ratner, J. Rzepiela, D. Schultz, T. Smith, P. Stefan, H. Tompkins, J. Turner, J. Welch, B. White, J. Wu, G. Yocky, R. Bionta, E. Ables, B. Abraham, C. Gardener, K. Fong, S. Friedrich, S. Hau-Riege, K. Kishiyama, T. McCarville, D. McMahon, M. McKernan, L. Ott, M. Pivovarov, J. Robinson, D. Ryutov, S. Shen, R. Soufli, and G. Pile, "Photon Beamlines and Diagnostics at LCLS," *Nucl. Instrum. Methods Phys. Res. A* **635**(1), S6–S11 (2011).
15. I. A. Vartanyants, A. Singer, A. P. Mancuso, O. M. Yefanov, A. Sakdinawat, Y. Liu, E. Bang, G. J. Williams, G. Cadenazzi, B. Abbey, H. Sinn, D. Attwood, K. A. Nugent, E. Weckert, T. Wang, D. Zhu, B. Wu, C. Graves, A. Scherz, J. J. Turner, W. F. Schlotter, M. Messerschmidt, J. Lüning, Y. Acremann, P. Heimann, D. C. Mancini, V. Joshi, J. Krzywinski, R. Soufli, M. Fernandez-Perea, S. Hau-Riege, A. G. Peele, Y. Feng, O. Krupin, S. Moeller, and W. Wurth, "Coherence Properties of Individual Femtosecond Pulses of an X-ray Free-Electron Laser," *Phys. Rev. Lett.* **107**(14), 144801 (2011).
16. P. Heimann, O. Krupin, W. F. Schlotter, J. J. Turner, J. Krzywinski, F. Sorgenfrei, M. Messerschmidt, D. Bernstein, J. Chalupský, V. Hájková, S. Hau-Riege, M. Holmes, L. Juha, N. Kelez, J. Lüning, D. Nordlund, M. F. Perea, A. Scherz, R. Soufli, W. Wurth, and M. Rowen, "Linac Coherent Light Source soft x-ray materials science instrument optical design and monochromator commissioning," *Rev. Sci. Instrum.* **82**(9), 093104 (2011).
17. J. Chalupsky, P. Bohacek, V. Hajkova, S. P. Hau-Riege, P. A. Heimann, L. Juha, J. Krzywinski, M. Messerschmidt, S. P. Moeller, B. Nagler, M. Rowen, W. F. Schlotter, M. L. Swiggers, and J. J. Turner, "Comparing different approaches to characterization of focused X-ray laser beams," *Nuc. Inst. and Meth. Phys. Res. Sec. A* **631**, 130–133 (2011).
18. M. Beye, O. Krupin, G. Hays, A. H. Reid, D. Rupp, S. de Jong, S. Lee, W.-S. Lee, Y.-D. Chuang, R. Coffee, J. P. Cryan, J. M. Glowina, A. Föhlisch, M. R. Holmes, A. R. Fry, W. E. White, C. Bostedt, A. O. Scherz, H. A. Durr, and W. F. Schlotter, "X-ray pulse preserving single-shot optical cross-correlation method for improved experimental temporal resolution," *Appl. Phys. Lett.* **100**(12), 121108 (2012).
19. I. H. Suzuki and N. Saito, "Y-value in rare gases for soft X-ray absolute measurement," *ETL Tech. Rep.* **56**, 688–711 (1992) (in Japanese).
20. N. Saito, private communication.
21. K. Tiedtke, J. Feldhaus, U. Hahn, U. Jastrow, T. Nunez, T. Tschentscher, S. Bobashev, A. Sorokin, J. Hastings, S. Moeller, L. Cibik, A. Gottwald, A. Hoehl, U. Kroth, M. Krumrey, H. Schoppe, G. Ulm, and M. Richter, "Gas detectors for x-ray lasers," *J. Appl. Phys.* **103**(9), 094511 (2008).
22. I. H. Suzuki and N. Saito, "Photoabsorption cross-section for Kr in the sub-keV energy region," *J. Electron Spectrosc. Relat. Phenom.* **123**(2-3), 239–245 (2002).
23. I. H. Suzuki and N. Saito, "Absolute photoabsorption cross-sections of Ne and Xe in the sub-keV X-ray region," *J. Electron Spectrosc. Relat. Phenom.* **129**(1), 71–79 (2003).
24. I. H. Suzuki and N. Saito, "Total photoabsorption cross-section of Ar in the sub-keV energy region," *Radiat. Phys. Chem.* **73**(1), 1–6 (2005).
25. N. Saito and I. H. Suzuki, "Precise photoabsorption cross sections of Ne and Xe," *Nucl. Instrum. Methods Phys. Res. A* **467–468**, 1577–1580 (2001).
26. L. Zheng, M. Cui, Y. Zhao, J. Zhao, and K. Chen, "Total photoionization cross-sections of Ar and Xe in the energy range of 2.1–6.0 keV," *J. Electron Spectrosc. Relat. Phenom.* **152**(3), 143–147 (2006).
27. B. L. Henke, E. M. Gullikson, and J. C. Davis, "X-ray Interactions: Photoabsorption, Scattering, Transmission, and Reflection at  $E = 50\text{--}30,000\text{ eV}$ ,  $Z = 1\text{--}92$ ," *At. Data Nucl. Data Tables* **54**(2), 181–342 (1993) (see also E. Gullikson., [http://www-cxro.lbl.gov/optical\\_constants/](http://www-cxro.lbl.gov/optical_constants/)).
28. B. Beckhoff, A. Gottwald, R. Klein, M. Krumrey, R. Müller, M. Richter, F. Scholze, R. Thornagel, and G. Ulm, "A quarter-century of metrology using synchrotron radiation by PTB in Berlin," *Phys. Status Solidi B* **246**(7), 1415–1434 (2009).
29. R. Soufli, M. Fernández-Perea, S. L. Baker, J. C. Robinson, E. M. Gullikson, P. Heimann, V. V. Yashchuk, W. R. McKinney, W. F. Schlotter, and M. Rowen, "Development and calibration of mirrors and gratings for the soft x-ray materials science beamline at the Linac Coherent Light Source free-electron laser," *Appl. Opt.* **51**(12), 2118–2128 (2012).
30. The respective dependence of the detection efficiency was obtained for low charge states during test measurements at the FLASH-FEL.
31. B. Schram, A. Boerboom, W. Kleine, and J. Kistemaker, "Amplification factors of a particle multiplier for multiply charged noble gas ions," *Physica* **32**(4), 749–761 (1966).
32. M. P. Stockli and D. Fry, "Analog gain of microchannel plates for 1.5–154 keV/ $q$   $\text{Ar}^{q+}$  ( $3 \leq q \leq 16$ )," *Rev. Sci. Instrum.* **68**(8), 3053–3060 (1997).
33. O. Krupin, M. Trigo, W. F. Schlotter, M. Beye, F. Sorgenfrei, J. J. Turner, D. A. Reis, N. Gerken, S. Lee, W. S. Lee, G. Hays, Y. Acremann, B. Abbey, R. Coffee, M. Messerschmidt, S. P. Hau-Riege, G. Lapertot, J. Lüning, P. Heimann, R. Soufli, M. Fernández-Perea, M. Rowen, M. Holmes, S. L. Molodtsov, A. Föhlisch, and W. Wurth, "Temporal cross-correlation of x-ray free electron and optical lasers using soft x-ray pulse induced transient reflectivity," *Opt. Express* **20**(10), 11396–11406 (2012).
34. V. Hájková, L. Juha, P. Bohacek, T. Burian, J. Chalupsky, L. Vysin, J. Gaudin, P. Heimann, S. Hau-Riege, M. Jurek, D. Klínger, J. Pelka, R. Sobierajski, J. Krzywinski, M. Messerschmidt, S. Moeller, B. Nagler, M. Rowen, W. Schlotter, M. Swiggers, J. Turner, S. Vinko, T. Whitcher, J. Wark, M. Matuchova, S. Bajt, H. Chapman, T.

- Dzelzainis, D. Riley, J. Andreasson, J. Hajdu, B. Iwan, N. Timneanu, K. Saksl, R. Faustlin, A. Singer, K. Tiedtke, S. Toleikis, I. Vartanians, and H. Wabnitz, "X-ray laser-induced ablation of lead compounds," Proc. SPIE **8077**, 807718 (2011).
35. R. Soufli, M. J. Pivovarov, S. L. Baker, J. C. Robinson, E. M. Gullikson, T. J. McCarville, P. M. Stefan, A. L. Aquila, J. Ayers, M. A. McKernan, and R. M. Bionta, "Development, characterization and experimental performance of x-ray optics for the LCLS free-electron laser," Proc. SPIE **7077**, 707716 (2008).
- 

## 1. Introduction

An impressive progress has been achieved in the development of powerful, next generation short-wavelength sources in the last few years, such as the self-amplified spontaneous-emission (SASE) free-electron laser (FEL) [1], enabling new investigations of photon-matter interactions on nanometer length and femtosecond time scales with ultra-high brightness. The recent advancement of this new generation of light sources has been a rapidly developing and exciting achievement for photon science. The free-electron laser in Hamburg (FLASH) at DESY operating in the extreme-ultraviolet (EUV) spectral range at wavelengths between 48 nm and 4.5 nm [2] was the first SASE driven FEL. The test accelerator EUV-FEL of the SPring-8 Compact SASE Source (SCSS) in Japan [3] was designed to demonstrate a compact FEL source and provides light pulses in the 51-61 nm wavelength range. The first x-ray FEL, the Linac Coherent Light Source (LCLS), was commissioned at the SLAC National Accelerator Laboratory in the United States, and operates at wavelengths between 1.5 nm and 0.15 nm [4], while FERMI in Trieste represents the first EUV-FEL with the so-called seeding scheme [5]. Finally, SACLA in Japan is the most recent machine to come on line and is the most compact FEL constructed to date [6]. Moreover, new X-ray FEL facilities in Europe (European XFEL), Korea (PAL-XFEL), Switzerland (SwissFEL) are currently under construction.

However, in spite of the progress in the development of these novel laser facilities, the characterization of FEL beam parameters such as the absolute photon flux, an important and fundamental quantity for many experiments, is a challenge. Existing methods such as calorimetry have been tested at an FEL before [7], but these intercept the beam and generally lack the required pulse resolution. Since each SASE-FEL pulse has a different number of photons, an on-line intensity monitoring of each pulse is needed. Another problem is that the peak power of the highly intense and strongly pulsed FEL beam (up to tens of gigawatts) can easily saturate or even destroy commonly used solid state detectors.

Using a gas-based transmissive measurement method mitigates these limitations and has the additional advantages that the wavefront of the coherent beam is preserved and that the gas target does not degrade with time as previously observed with solid state absorbers or beam splitters. It has a larger dynamic range, and can be placed in front of or close to the sample and thus measure the number of photons per pulse directly at the sample location.

With the commissioning of the LCLS, one open question was if pulse energies could be determined reliably from bursts of x-rays that were orders of magnitude higher than those found at other FEL facilities. In addition to the hard x-ray regime, the facility also hosts the world's only FEL source of soft x-rays. These are energies in the range of about 280 eV – 2 keV where spectroscopy, diffraction and imaging are used to study atomic, molecular, and optical physics [8] as well as chemistry and condensed matter [9]. Absolute detection of the photon number per pulse had previously only occurred using longer wavelength radiation [10], and in the hard X-ray regime [11], both with different repetition rate time structures. The question arises whether existing technology can be used to measure pulse energies under these new conditions.

This paper demonstrates that high intensity, short-pulse soft x-ray bursts can be measured at a FEL facility on an absolute scale. We measure the radiant power and, hence, the full beamline transmission by using an absolute detector temporarily placed at the end of the instrument. This also provides an estimate of the photon number per bandwidth.

## 2. Background

In order to overcome the challenges associated with photon flux measurements at FEL sources, different detection techniques have been developed. At FLASH, the pulse resolved radiant power is measured on-line and non-destructively using permanently installed calibrated gas-monitor detectors (GMDs) developed in close cooperation between DESY, PTB, and Ioffe Institute [10]. The detector is based on the atomic photoionization of rare gases at low pressures and the charge detection of photo-ions and photoelectrons by Faraday cups. At LCLS, a different kind of gas detector based on the photoluminescence in nitrogen at a high pressure on the order of 1 mbar [12] is used. In order to ensure the accuracy of different detection schemes, a successful comparison was performed at SCSS between a new stand-alone upgrade of the FLASH-GMD, the so-called Transfer-GMD, and the AIST cryogenic radiometer at the wavelengths of 51 nm, 56 nm, and 61 nm, revealing that radiant power values obtained with the two different detectors agree to within 2.6%, with their combined relative standard uncertainty being 4.5% [13]. A similar comparison was recently performed at SACLA in the hard X-ray regime [11].

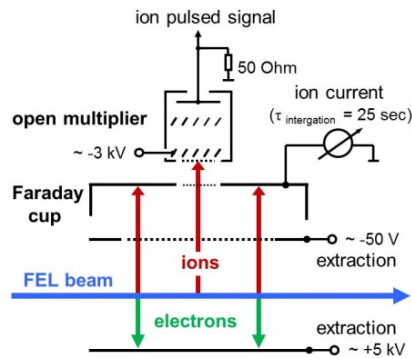


Fig. 1. Schematic diagram of the gas monitor detector built by DESY, PTB, and Ioffe. The blue arrow represents the photon beam, while red and green represent the direction of ion and electron beam trajectories, respectively.

The Transfer-GMD was brought to LCLS as part of the initial commissioning [14] of the Soft X-ray Materials Studies (SXR) instrument [9] at the LCLS [4], an instrument which delivers coherent [15] soft x-ray radiation, via a monochromator [16], a Kirkpatrick-Baez (KB) focusing mirror system [17], and a suite of timing diagnostics [18] for precise pulse arrival. Figure 1 depicts a scheme of the Transfer-GMD. As in the previous version of the GMD operated in the EUV range [10], ions and electrons created by the photoionization of a target gas at a low pressure of  $10^{-2}$  Pa to  $10^{-4}$  Pa are separated and extracted from the interaction volume by a homogeneous static electric field. The extraction field of a few kV is high enough to ensure the complete collection of the ions created in the interaction volume and their detection is by a simple metal electrode (Faraday cup) in order to guarantee a linear signal response. A Faraday cup is a metal conductor designed in a particular shape to capture charged particles in vacuum, where the final current measurement can be used to determine the number of ions hitting the cup. Furthermore, a fraction of ions pass through a slit in this Faraday cup in the upgraded version of the GMD, and may alternatively be detected by an open electron multiplier with an amplification factor of up to  $10^6$ . This feature makes the device sufficiently sensitive for the soft X-ray regime as well, where the atomic photoionization cross-sections are orders of magnitude smaller than in the EUV spectral range. The open multiplier for the ions can also be used to measure the ions' time-of-flight (TOF) spectrum and thus to distinguish different ion charge states. These spectra provide insight into the spectral purity of FEL radiation as well as yield information about the mean

ion charge. The latter is necessary to determine the photon flux. The measurements can be performed in a pulse-resolved mode and in addition, the GMD provides a slowly averaging ion-current from the Faraday cup with a time constant of up to 30 s, which is not affected by any time structure of the radiation.

### 3. Theory

The number of photons  $N_{\text{photon}}$  passing through the detector is determined by the number of detected ions  $N_{\text{ion}}$  by:

$$N_{\text{photon}} = \frac{N_{\text{ion}}}{Q \cdot E(\hbar\omega)} = \frac{N_{\text{ion}}}{\sigma(\hbar\omega) \cdot z \cdot \eta \cdot n \cdot K_{\text{amp}}} \quad (1)$$

In Eq. (1),  $Q \cdot E(\hbar\omega)$  is the quantum efficiency at the photon energy  $\hbar\omega$  which is proportional to the total photoionization cross section  $\sigma(\hbar\omega)$ . The length  $z$  is the distance along the photon beam accepted by the respective ion detector,  $\eta$  is the ion detection efficiency,  $n$  is the density of target gas atoms, and  $K_{\text{amp}}$  is the amplification factor of the respective ion detector which is equal to unity for the Faraday cup. The gas atomic density is obtained according to the equation  $n = p/k_B T$ , where  $k_B$  is the Boltzmann constant,  $p$  is the gas pressure determined using a calibrated spinning rotor gauge, and  $T$  is the temperature measured by a calibrated Pt100 resistance thermometer. The number  $N_{\text{ion}}$  is determined through the charge  $Q$  accumulated by the respective particle detector with  $N_{\text{particle}} = Q/eq(\hbar\omega)$ , where  $e$  is the elementary charge and  $q(\hbar\omega)$  is the ion mean charge which can be deduced from the measured ion TOF spectrum or in some cases (for photon energies up to 1200 eV) taken from the literature [19, 20]. Since the total photoionization cross sections are well known from the literature [20–27], the product  $z \cdot \eta$  is the only factor that is determined by calibration.

### 4. Experimental

The GMD was calibrated in the ion-current mode at the PTB laboratory at the Metrology Light Source (MLS) by using dispersed synchrotron radiation in the vacuum-ultraviolet (VUV) spectral range at intensities of a few microwatts. For the absolute photon flux measurements, a semiconductor photodiode calibrated with a cryogenic radiometer was used as a secondary standard source of calibration [28]. Figure 2 shows the measured quantum efficiency for the slow ion-current signal of the GMD, operated with xenon as the target gas, in the photon energy range from 14 eV to 31 eV. The data is normalized to the atomic particle density. Since the dependence on the photon energy ( $\hbar\omega$ ) of the normalized quantum efficiency of the detector is dominated by the total photoionization cross sections, the latter values taken from previous work [20–27] have been used to extrapolate the measured data from 14 eV to X-rays (~13 keV) for neon (Ne), argon (Ar), krypton (Kr), and xenon (Xe) as the target gas. Gaps in the calibration curves indicate spectral regions where the extrapolation is complicated by the presence of auto-ionization resonances and thresholds. The overall relative standard uncertainty for the calibration curves is below 6% (see section 5.3).

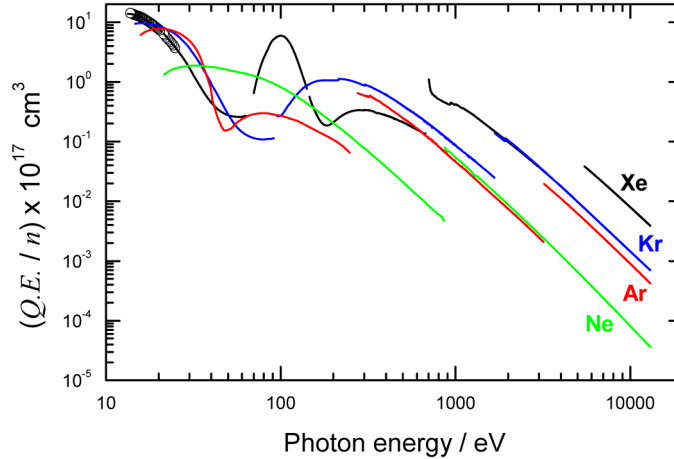


Fig. 2. Quantum efficiency of the photo-ion current signal of the GMD operated with neon, argon, krypton, and xenon, and normalized to the particle density. The circles represent the measurements while the solid lines are an extrapolation calculated using total photoionization cross-sections.

## 5. Results

Pulse intensity measurements were carried out in the photon energy range between 540 eV and 2000 eV using FEL radiation at the SXR beamline [9] of the LCLS. The photon pulse repetition rate was 60 Hz. The LCLS has two gas detectors for monitoring the pulse energy placed upstream and downstream of the FEL beam attenuator in the front end enclosure (FEE) [12]. The SXR beamline has seven x-ray optical elements along the instrument downstream of the LCLS gas detectors. All optical elements have been coated with a special B<sub>4</sub>C layer applied to silicon substrates to handle the large pulse energies [29]. The detection efficiency of the LCLS detectors was estimated by a method based on the measured energy loss of the electrons passing through the undulator. After absolute scale calibration, the Transfer-GMD was placed at the beamline endstation position downstream of all optical elements, including the K-B focusing mirrors. Hence, by comparing radiant power measured by all three detectors, both the beamline transmission as well as the linearity of the detectors could be obtained.

The Transfer-GMD was operated using Kr and Xe as target gases. In order to check both the purity of the gases as well as the quality of the detector vacuum, a series of ion time-of-flight (TOF) spectra averaged over 1000 photon pulses was measured at different photon energies. As an example, Fig. 3 shows spectra of Kr and Xe taken at a photon energy of 800 eV. In both cases a clear progression of the rare gas ion charge states can be seen with only a minute peak due to hydrogen indicating very clean gas and vacuum conditions.

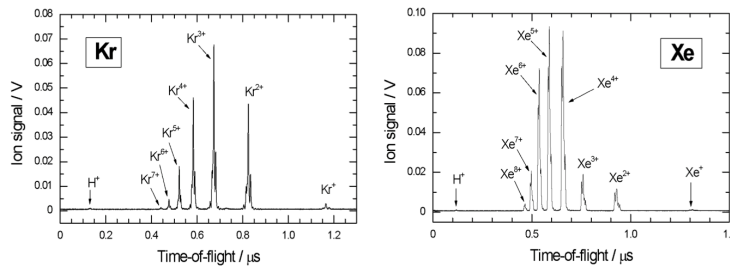


Fig. 3. Ion TOF spectrum of both Kr and Xe taken at the photon energy of 800 eV.

### 5.1 Spectral purity

The TOF spectra can also be used as a diagnostic tool to investigate the spectral purity of the FEL radiation. Higher harmonic content of the FEL fundamental energy is usually present at about a few percent, in addition to potential spontaneous undulator radiation, which can contribute to excess radiation measured with the GMD. For this purpose, the ratios of the partial photoionization cross sections for different charged ions and the ion mean charges were deduced from the TOF spectra and compared with those known from the literature. The individual ion peaks have been integrated and corrected with respect to the charge dependence of the multiplier detection efficiency. The latter was assumed to be proportional to the ion impact velocity [30–32].

**Table 1. Branching ratios of partial cross-sections for different ionic charge states  $i$  and ion mean charges  $q$  of Xe and Kr measured by the Transfer-GMD during the SXR commissioning together with those quoted from the literature [19, 20].**

Photon energy / eV	Gas	Branching ratio and ion mean charge $q$	SXR measurements	Literature data
800	Xe	$\sigma^{2+} / \sigma^{5+}$	$0.24 \pm 0.03$	0.238
		$\sigma^{3+} / \sigma^{5+}$	$0.28 \pm 0.04$	0.263
		$\sigma^{4+} / \sigma^{5+}$	$1.19 \pm 0.15$	1.22
		$\sigma^{6+} / \sigma^{5+}$	$0.63 \pm 0.08$	0.594
		$\sigma^{7+} / \sigma^{5+}$	$0.14 \pm 0.02$	0.127
		$\sigma^{8+} / \sigma^{5+}$	$0.022 \pm 0.004$	0.014
		$q = \sum_i i \sigma^{i+} / \sum \sigma^{i+}$	$4.6 \pm 0.3$	$4.52 \pm 0.07$
800	Kr	$\sigma^{+} / \sigma^{3+}$	$0.08 \pm 0.02$	0.076
		$\sigma^{2+} / \sigma^{3+}$	$0.8 \pm 0.1$	0.77
		$\sigma^{4+} / \sigma^{3+}$	$0.52 \pm 0.07$	0.508
		$\sigma^{5+} / \sigma^{3+}$	$0.16 \pm 0.02$	0.159
		$\sigma^{6+} / \sigma^{3+}$	$0.032 \pm 0.005$	0.034
				$q = \sum_i i \sigma^{i+} / \sum \sigma^{i+}$
1200	Xe	$\sigma^{2+} / \sigma^{5+}$	$0.23 \pm 0.03$	0.234
		$\sigma^{3+} / \sigma^{5+}$	$0.23 \pm 0.03$	0.240
		$\sigma^{4+} / \sigma^{5+}$	$1.13 \pm 0.16$	1.15
		$\sigma^{6+} / \sigma^{5+}$	$0.88 \pm 0.12$	0.84
		$\sigma^{7+} / \sigma^{5+}$	$0.52 \pm 0.07$	0.44
		$\sigma^{8+} / \sigma^{5+}$	$0.26 \pm 0.04$	0.18
		$q = \sum_i i \sigma^{i+} / \sum \sigma^{i+}$	$5.1 \pm 0.4$	$4.95 \pm 0.07$
1200	Kr	$\sigma^{+} / \sigma^{3+}$	$0.09 \pm 0.02$	0.0588
		$\sigma^{2+} / \sigma^{3+}$	$0.62 \pm 0.09$	0.578
		$\sigma^{4+} / \sigma^{3+}$	$0.63 \pm 0.09$	0.647
		$\sigma^{5+} / \sigma^{3+}$	$0.20 \pm 0.03$	0.176
		$\sigma^{6+} / \sigma^{3+}$	$0.040 \pm 0.007$	0.0392
				$q = \sum_i i \sigma^{i+} / \sum \sigma^{i+}$

Table 1 shows some ratios of partial cross sections for different ionic charge states and ion mean charge measured at photon energies of 800 eV and 1200 eV. For these types of measurements, the beamline monochromator was set to zero-order mode [33], defined here as the reflection from the un-ruled portion of the monochromator grating. The data were obtained while the LCLS attenuator was filled with nitrogen with a transmission of about 20%. Good agreement between the present data and the literature, especially for the ion mean charges, clearly demonstrates that the GMD signals were not significantly affected by either FEL higher order components or spontaneous undulator radiation. Nevertheless, an attenuator



can absorb not only the fundamental, but also the spontaneous undulator radiation depending on the spectral range, reducing the contribution of the latter to the GMD signal. In order to understand this we performed measurements of the ratios and the mean charge as a function of the pressure (or transmission) in the attenuator. This is exemplified in Fig. 4 for a data set on Xe at different attenuator transmissions. The ratios and the mean charge remained constant within 2% to 10% which is close to the measurement uncertainties. Therefore, we can conclude that the photon flux measured with the GMD is not substantially affected by any additional radiation from photon energies different than that of the fundamental.

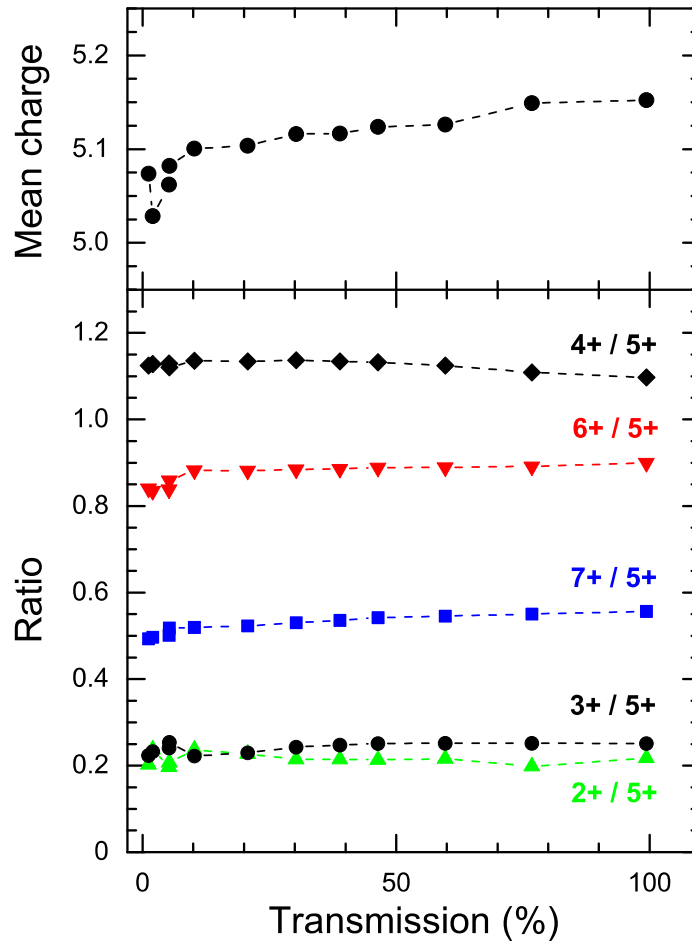


Fig. 4. Ratios of partial cross-sections for different charge states and the ion mean charge of Xe as a function of the attenuator transmission at a photon energy of 1200 eV. The negligible slope demonstrates the spectral purity and lack of contamination from higher harmonics and spontaneous optical radiation from the undulator.

### 5.2 Linearity

The comparison of the average radiant power over many shots is measured by both the LCLS detectors and the Transfer-GMD for different photon intensities and can be used to evaluate the linearity of the LCLS detectors. Figure 5(a) shows an averaged pulse energy obtained by the LCLS detector as a function of those measured by the GMD. Since the latter has been calibrated on an absolute scale and was obtained by measuring the ion current from the

Faraday cup, the signal from the GMD is assumed to be linear with intensity. Under this assumption, any deviation between the two data sets at high pulse energies indicates a non-linear behavior of the LCLS detector. From the correlation plot it can be seen that the LCLS detector remained linear up to pulse energies of about  $\sim 1.75$  mJ. For the SASE mode of the LCLS, the majority of experiments operate in this range. In Fig. 5(b), the relationship of the transmission of the gas attenuator to the GMD signal is shown to be linear over the whole range up to the measured value of 0.8 mJ, confirming the low pulse energy linearity of the relative monitors. The GMD calibration allows for a monotonic correction to the LCLS gas detector signal, in order to obtain a calibrated absolute flux.

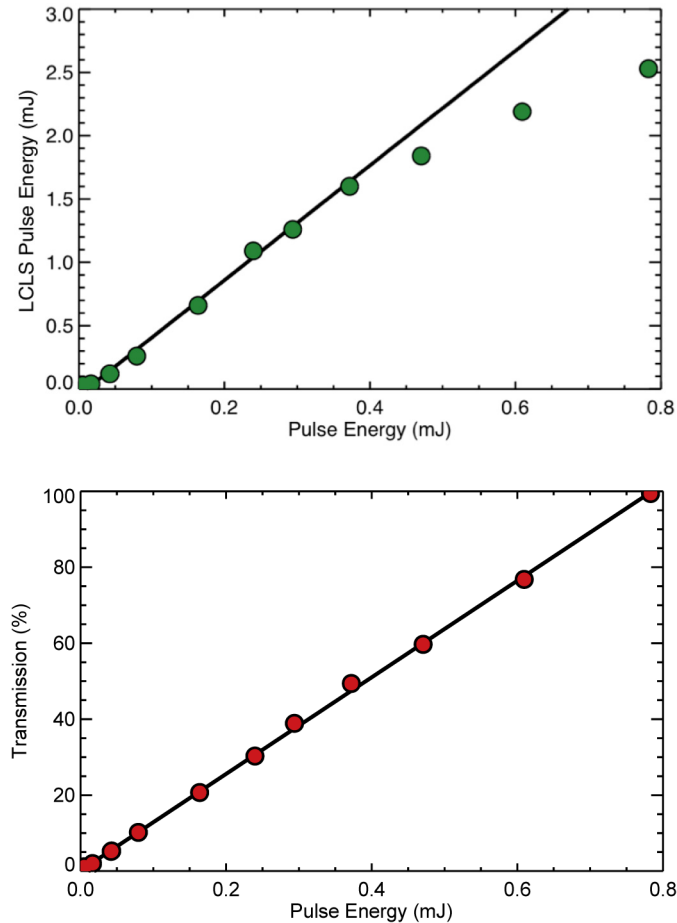


Fig. 5. (a) Average photon pulse energy over multiple shots measured by the LCLS gas detector versus those obtained with the GMD placed after all x-ray optical elements at 1200 eV. The LCLS gas detectors are shown to be linear up to about  $\sim 1.75$  mJ. (b) Transmission of the gas attenuator vs. GMD signal showing linear behavior over the whole range measured.

### 5.3 Soft X-ray transmission

As noted above, the GMD has been calibrated absolutely in the VUV spectral range with Xe as a target gas, and published photoionization cross sections of rare gases have been used to extrapolate the calibration to a higher photon energy range. In the spectral range of the present investigation, the cross section of Xe and Kr differ by an order of magnitude. In order to validate our measurements, we determined pulse energies with both Xe and Kr used as the target gas for the GMD. As an example, Table 2 depicts the average pulse energy at a photon

energy of 800 eV measured by the GMD in the current mode with different target gases. The attenuator setting was 20% and the zero-order radiation from the monochromator was utilized. Both target gases yield the same values within the uncertainty of the measurement. This close agreement validates our measurement methodology.

**Table 2. Average energy of the photon pulses measured by the Transfer-GMD operated with both Xe and Kr as the target gas. Both gases yield comparable numbers. This allows for the total transmission of the SXR instrument to be obtained by comparison with the LCLS gas detector.**

Photon energy (eV)	Target gas	Attenuator transmission (%)	Pulse Energy (GMD) (mJ)	Beamline transmission (%)
800	Xe	20	$0.068 \pm 0.004$	$23 \pm 2$
800	Kr	20	$0.065 \pm 0.004$	$21 \pm 2$

Furthermore, the values of the two different target gases could also be compared with the pulse energy measured by the LCLS detector located upstream of the attenuator. This enabled us to determine the SXR instrument transmission of about 22%. The relative standard uncertainty of the determined pulse energy is 6% which is obtained by a standard error propagation of products in Eq. (1) and is due to the uncertainties of the following quantities: the product  $z \cdot \eta$  at 3.4%, the pressure measurement at 1.5%, the temperature measurement at 1%, the photoionization cross sections at 2.5%, the mean charge at 2%, and the ion current measurement at 3%. The uncertainty of the transmission values combines the uncertainty of the pulse energy measured by the GMD and the statistical fluctuation of the signal taken from the LCLS detector. A good agreement between the values given in Table 1 confirms the reliability of the photon flux measurements performed by the Transfer-GMD. Moreover, single-shot ablation thresholds of selected high-Z high-density materials [17], which strongly absorb the LCLS radiation, were determined by means of LCLS pulse energy distributions. Other threshold values [34] obtained during the commissioning validated the Transfer-GMD measurements as well.

Figure 6 shows the transmission of the SXR instrument for different photon energies, summarizing the comparison of the FEL average pulse energy measured by the Transfer-GMD and the LCLS gas detectors. The values are obtained by averaging measurements performed with different target gases in the GMD as well as different attenuator transmissions varying from 1% to 100%. The measured transmittance for the 0th order appears to be consistently lower than the estimated values, by between 10 and 15%. Expected values are shown (grey lines) and are based on calculations using measured reflectivities and diffraction efficiencies for each of the seven boron carbide-coated elements in the beam path, i.e: three mirrors and one grating in the SXR beamline and three additional mirrors upstream of the beamline in the FEE [35]. We have used the calculated values (grey line) for the zeroth order numbers to show the agreement on the trend of the data with energy, but have scaled it down to make interpolation between energies easier. The first order trend (grey line) shows the exact calculated values for the 100 l/mm grating without scaling. The 800 eV agrees very well, and the 1200 eV is roughly a factor of two lower than expected. Unfortunately, the two first order data points were all that was allowed by the time constraints of the experiment. To understand more carefully the trend of the first order data, a follow-up paper will detail both the 100 l/mm and 200 l/mm gratings over the full energy spectrum. The origin of the discrepancies in the zero order measurements observed in Fig. 6 might be due to a steering misalignment of the FEL beam, lower than expected reflectivity for some of the mirrors due to aging effects, or to a non-linearity from the LCLS detectors. Also the calibration of the LCLS detectors based on the ‘electron energy loss’ method provides only an upper limit of the photon pulse energy, resulting in a lower limit for the beamline transmission.

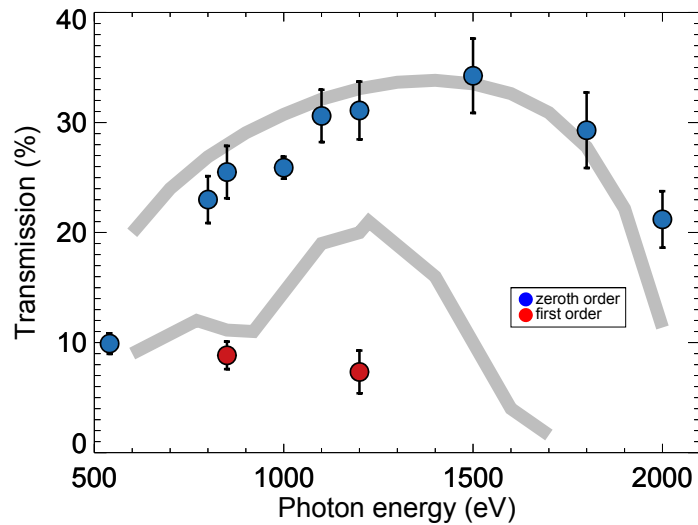


Fig. 6. Measured transmission of the SXR instrument for both zero-order and 1st-order settings of the 100 l/mm grating of the beamline monochromator as a function of the x-ray energy. The expected values of the first order and the zeroth order (scaled) are also shown in grey for comparison, except for 540 eV. Estimating the transmission near 540 eV (the oxygen K edge) would be very challenging due to the possibility of an undetermined amount of oxide having formed on the top surface of some of the mirrors.

#### 5.4 Photon radiation energy resolution

Finally, another important metric was obtained using the Transfer-GMD device: to precisely measure the photon pulse energy as a function of the photon bandwidth. This information is vital to the operation of FEL experiments, especially in materials studies, as it displays the trade-offs between photons delivered to a given experiment and the bandwidth of those soft x-ray photons. The photon flux versus bandwidth relationship was obtained by measuring the pulse energy as a function of exit slit opening of the SXR monochromator. Figure 7 shows the percentage of photons that reach the sample as a function of photon bandwidth using the Transfer-GMD. The FEE gas detector was used to calibrate the initial photon number for 540 eV radiation, shown with blue data points. The black lines are the calculated percentage of photons for 800 eV (dashed) and 1500 eV (dotted), respectively, using the known bandwidth change with energy of the FEL, the grating efficiency [29], and the measured dispersion of the grating [16]. Note that this energy calculation includes the estimated losses along the accelerator due to the much longer wavelengths used than what the LCLS was originally designed to provide for the lowest energies over the soft x-ray range.

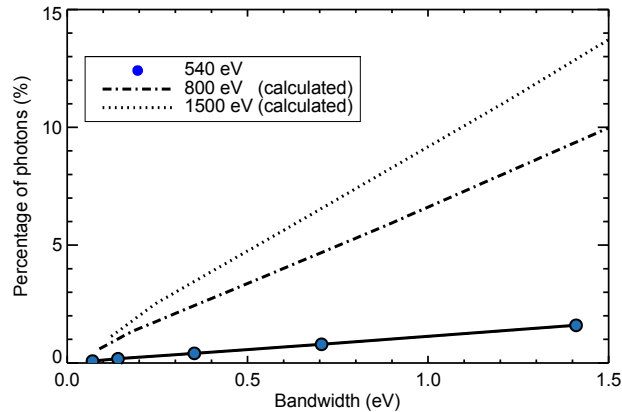


Fig. 7. The percentage of photons transmitted to the sample through the monochromator at the SXR instrument for the 100 l/mm grating as a function of bandwidth. The blue data points are for measured data at 540 eV. The black dashed and dotted lines are calculated from the data for 800 eV and 1500 eV, respectively.

## 6. Summary

In conclusion, we successfully performed novel radiation measurements of the FEL pulse energy in the soft x-ray regime at the Linac Coherent Light Source on an absolute scale. These measurements clearly demonstrate that the GMD signals are not affected by higher harmonics or spontaneous undulator radiation, which has a broad spectral distribution ranging from the VUV to the hard x-ray regime. Thus, gas detectors based on atomic photoionization are well suited for photon diagnostics at the existing or upcoming large x-ray laser facilities like LCLS, Spring-8, and the European XFEL. The comparative measurements with the LCLS gas detectors were performed and allowed us to determine their linearity and in addition, the full SXR instrument transmission through multiple x-ray optical elements. These experimental transmission values range from 10% to 34%. We also measured pulse energies as a function of photon bandwidth by recording transmission through the exit slit of the monochromator. This allows the relationship between photon number and energy resolution to be accurately determined, an important metric for future FEL experiments that use monochromatic radiation in the soft x-ray range.

## Acknowledgments

Portions of this research were carried out on the SXR Instrument on the Linac Coherent Light Source (LCLS) at the SLAC National Accelerator Laboratory. The SXR Instrument is funded by a consortium whose membership include the LCLS, Stanford University through the Stanford Institute for Materials Energy Sciences (SIMES), Lawrence Berkeley National Laboratory (LBNL), University of Hamburg through the BMBF priority program FSP 301, and the Center for Free Electron Laser Science (CFEL). The LCLS is funded by the U.S. Department of Energy's Office of Basic Energy Sciences. This work was also performed under the auspices of the U.S. Department of Energy by Lawrence Livermore National Laboratory under Contract No. DE-AC52-07NA27344. Financial support for Mónica Fernández-Perea was provided in part by Ministerio de Educacion y Ciencia, Programa Nacional de Movilidad de Recursos Humanos del Plan nacional de I + D + I 2008-2011. We acknowledge the support of I.A. Vartaniants, A.P. Mancuso, O.M. Yefanov and A. Singer from DESY, B. Abbey from La Trobe University, and the SXR commissioning team for support during commissioning of the SXR instrument. We also wish to acknowledge the Czech Ministry of Education for financial support within the program INGO (project LG13029).